NO_x-catalyzed gas-phase activation of methane: *in situ* IR and mechanistic studies

Zhen Yan, Chao-Xian Xiao, and Yuan Kou *
College of Chemistry and Molecular Engineering, Peking University, Beijing 100871, China

Received 17 July 2002; accepted 4 October 2002

The products of reactions occurring in a CH_4–O_2–NO_x mixture have been investigated by *in situ* FTIR spectroscopy. The results show that low temperatures favor the formation of HCHO and CH_3OH, while high temperatures favor that of C_2H_4. Possible reaction mechanisms based on the *in situ* observations are briefly discussed.

KEY WORDS: gas-phase oxidation; methane activation; NO_x; *in situ* FTIR spectroscopy; mechanism.

1. Introduction

There have been many *in situ* IR studies of catalytic activation of methane over solid catalysts, but little attention has been paid to any simultaneous gas-phase reactions involved. *In situ* IR studies of gas-phase catalytic activation of methane have been rarely reported. NO_x-catalyzed gas-phase activation of methane [1–11] has many advantages as far as performing an *in situ* IR study is concerned. The absence of a solid catalyst, together with the high IR sensitivities of the different products, means that *in situ* observations can be carried out with either very low or very high methane concentrations, over a very wide temperature range. Furthermore, since the nature of the product mixture obtained from the activation of methane over a solid catalyst is believed to be dependent on the surface structure of the latter, an *in situ* IR study of the NO_x-catalyzed gas-phase reaction may provide an excellent reference point for comparing what is occurring on different surfaces.

In a previous paper, we have shown that NO_x is a good catalyst for the oxidation of methane [12]. The products obtained are mainly CO, H_2, HCHO/CH_3OH, and C_2H_4/aromatics. In this paper we report *in situ* IR experiments that allow us to study the formation of each of the products in detail. Possible reaction mechanisms based on our *in situ* observations are briefly discussed.

2. Experimental

The *in situ* experiments were carried out in a home-made stainless steel infrared cell with quartz walls (i.d. 9 mm) and a 15 cm path length. KBr windows cooled by flowing water were used. An 8 cm heating element wrapped around the cell allowed collection of *in situ* spectra at elevated temperatures. The temperature was monitored by means of a thermocouple located on the outside of the cell and was calibrated by another thermocouple put in the cell under the same conditions. The gases were controlled by mass flow controllers and premixed before entering the cell. *In situ* infrared spectra were collected using a Bruker Vector 22 spectrometer with a resolution of $2\,cm^{-1}$. Reference spectra were collected by flowing N_2 through the cell at the same temperature and flow rate as in the corresponding reactions. The absorption due to water in some spectra was subtracted.

3. Results and discussion

3.1. In situ IR study

Figure 1 shows the *in situ* infrared spectrum of the 20% CH_4–10% O_2–0.06% NO system at 600 °C. Absorption peaks due to CO_2 ($2390–2280\,cm^{-1}$), CO ($2250–2000\,cm^{-1}$), HCHO ($1745\,cm^{-1}$), CH_3OH ($1033\,cm^{-1}$), and C_2H_4 ($949\,cm^{-1}$) can be observed.

In situ FTIR investigation shows that the amount of each product formed varies significantly with the reaction conditions. The most important variable is the reaction temperature. With the conditions shown in figure 2, formation of HCHO is observed at 460 °C, and subsequently CO (at 470 °C), CH_3OH (at 480 °C), and C_2H_4 (at 520 °C) are observed with increasing temperature. The concentration of CO increases with temperature, and reaches a maximum between 650 and 750 °C, and then begins to decrease. The amounts of HCHO and CH_3OH both reach maxima at 540 °C, and

---

* To whom correspondence should be addressed.
E-mail: yuankou@pku.edu.cn

1011-372X/03/0200-0135/0 © 2003 Plenum Publishing Corporation

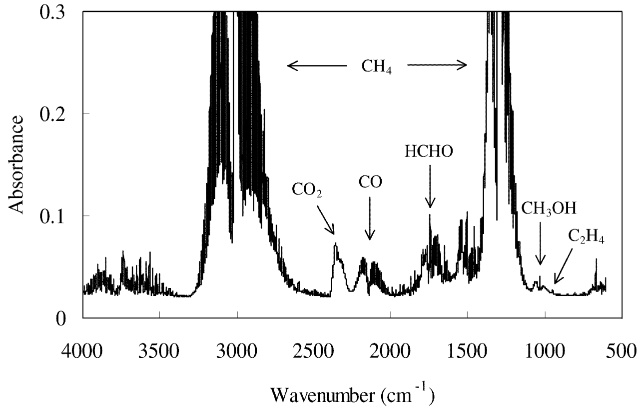

Figure 1. *In situ* FTIR spectrum. Reaction conditions: CH_4, 20%; O_2, 10%; NO, 0.06%; flow rate, 120 ml/min; 600 °C.

then decrease, but HCHO can be observed until 800 °C, while CH_3OH becomes undetectable above 720 °C. The amount of C_2H_4 increases monotonically with temperature. It can be seen from figure 2 that low temperatures favor the formation of HCHO and CH_3OH, while high temperatures favor that of C_2H_4.

In comparison with reaction temperature, the CH_4/O_2 ratio and the flow rate have less significant effects on the product distributions. Elevated temperatures are required to bring about reaction for high CH_4/O_2 ratios or flow rates. Lower amounts of HCHO and CH_3OH are formed at low flow rates, which means HCHO and CH_3OH are oxidized to CO_x when reaction times are longer.

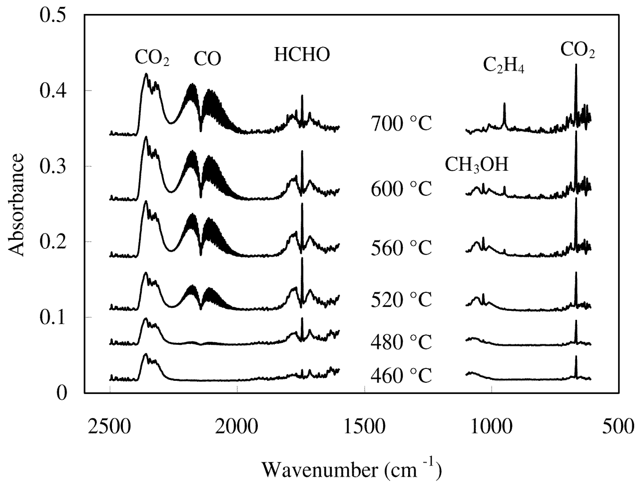

Figure 2. *In situ* IR spectra of the CH_4–O_2–NO_x system at different temperatures. Reaction conditions: CH_4, 20%; O_2, 10%; NO, 600 ppm; N_2, balance; flow rate, 80 ml/min.

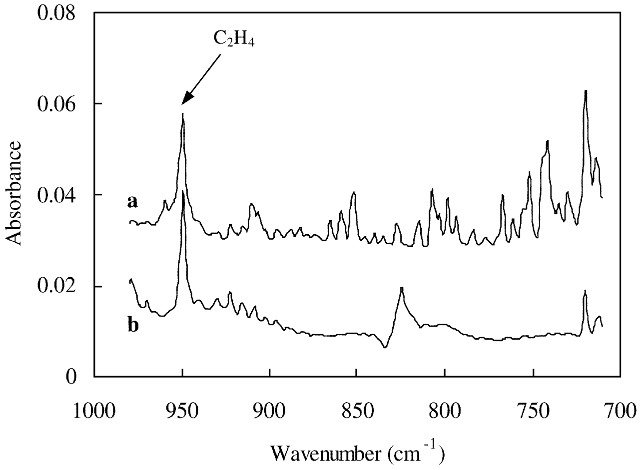

Figure 3. *In situ* FTIR spectrum (a) and on-line FTIR spectrum (b). Reaction conditions: CH_4, 20%; O_2, 10%; NO, 0.06%; flow rate, 40 ml/min; 600 °C.

The *in situ* IR spectra have been compared with the on-line spectra, which were measured at room temperature by flowing the product gas into a 10 cm long gas cell. The absorption peaks due to the main products (CO_2, CO, HCHO, CH_3OH, C_2H_4) observed *in situ* are consistent with those obtained on-line, but the *in situ* measurements are more sensitive than the on-line ones, for which products can only be observed at reaction temperatures higher than 500 °C. For example, the formation of HCHO is first observed at 520 °C in the on-line experiments. However, this temperature actually represents the temperature where the maximum amount of HCHO is formed. The temperature at the onset of formation is in fact 460 °C from the *in situ* observations. Some weak absorptions, which are absent from the on-line spectra, are observed in the 1000–700 cm^{-1} region of the *in situ* spectra when the reaction is carried out at higher temperatures, as shown in figure 3.

The infrared absorptions at 870–850 cm^{-1} and 810–790 cm^{-1} may be due to *cis*-HONO and *trans*-HONO, respectively [13]. These absorptions have been theoretically predicted, but not experimentally observed, by both McConkey and Wilkinson [2] and Tabata *et al.* [9]. To validate this prediction, a series of parallel experiments were carried out. *In situ* IR observations of CH_4–O_2, CH_4–NO, and NO–O_2 co-feed systems under the same reaction conditions were performed, but no signals in the above regions were detected. On the other hand, when CH_4 was substituted by H_2, and the H_2–O_2–NO system was examined, these absorption peaks were observed. These results, shown in figure 4, demonstrate that the weak absorptions (*) are indeed due to the N–O stretching vibrations of HONO.

3.2. Mechanism

Two mechanisms for the reactions in the $CH_4 + O_2 + NO_x$ systems are often cited in the literature. McConkey and Wilkinson [2] proposed the following reaction mechanism:

$$NO + CH_4 \rightarrow HNO\cdot + CH_3\cdot$$

or

$$2NO + O_2 \rightarrow 2NO_2$$

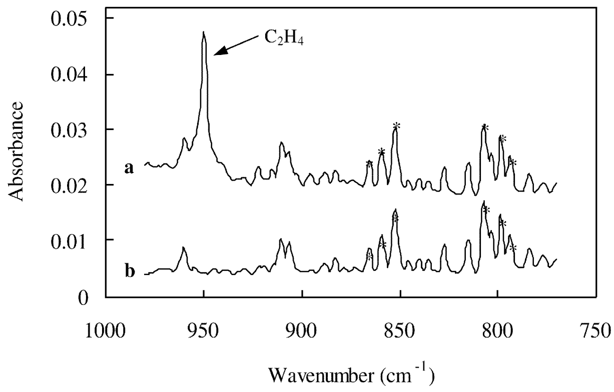

Figure 4. *In situ* FTIR spectra of CH_4–O_2–NO (a) and H_2–O_2–NO (b). The asterisks indicate NO stretching vibrations of HONO.

and

$$NO_2 + CH_4 \rightarrow HNO_2 + CH_3\cdot$$
$$O_2 + HNO\cdot \rightarrow OH\cdot + NO_2$$
$$O_2 + HNO\cdot \rightarrow HO_2\cdot + NO$$

Methane is subsequently oxidized to formaldehyde by the following pathway:

$$OH\cdot + CH_4 \rightarrow H_2O + CH_3\cdot$$
$$HO_2\cdot + CH_4 \rightarrow H_2O_2 + CH_3\cdot$$
$$CH_3\cdot + O_2 \rightarrow H_2CO + OH\cdot$$

Tabata *et al.* [9] calculated the transition barriers of various reactions involving $CH_4 + O_2 + NO_x$ and suggested the following reaction model:

$$NO_2 + CH_4 \rightarrow HNO_2 + CH_3\cdot$$
$$NO_2 + CH_4 \rightarrow trans\text{-}HONO + CH_3\cdot$$
$$CH_3\cdot + NO_2 \rightarrow CH_3NO_2$$
$$CH_3\cdot + NO_2 \rightarrow trans\text{-}CH_3ONO$$
$$trans\text{-}CH_3ONO \rightarrow CH_3O\cdot + NO$$
$$CH_3O\cdot + CH_4 \rightarrow CH_3OH + CH_3\cdot$$

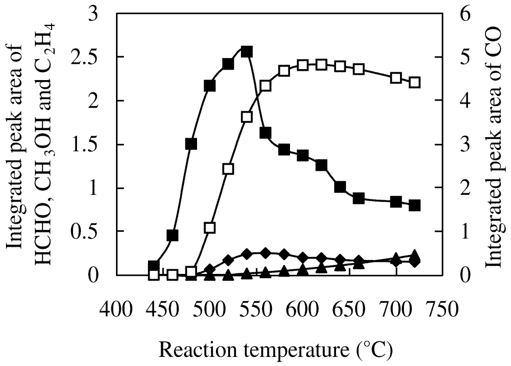

Figure 5. Variation of integrated peak area with reaction temperature for CH_2O ($\nu = 1745\,cm^{-1}$, ■), CH_3OH ($\nu = 1033\,cm^{-1}$, ●), C_2H_4 ($\nu = 950\,cm^{-1}$, ▲), and CO ($\nu = 2200\,cm^{-1}$, □). Reaction conditions: CH_4, 20%; O_2, 10%; NO, 600 ppm; N_2, balance; flow rate, 80 ml/min.

$$CH_3O\cdot \rightarrow HCHO + H\cdot$$
$$CH_3O\cdot + O_2 \rightarrow HCHO + HO_2$$
$$CH_3O\cdot + NO_2 \rightarrow HCHO + HNO_2$$
$$CH_3O\cdot + NO \rightarrow HCHO + HNO$$

These mechanisms suggest that methane may be activated by either NO or NO_2. The appearance of HNO_2 signals would clearly indicate the pathway initiated by NO_2, since CH_4 may react with NO_2 to produce CH_3 and HNO_2. HNO_2 is unstable at room temperature and decomposes via the following reaction:

$$2HONO \rightarrow NO + NO_2 + H_2O$$

This may be the reason that no HNO_2 absorption is observed in our on-line IR spectra. Under the same reaction conditions, the fact that the CH_4–NO system also gives no similar absorption in this region provides further evidence to support the conclusion that the activation of methane is initiated by NO_2.

The variations in product concentration (based on IR peak area) with reaction temperature observed in our experiments (figure 5) are partly consistent with the

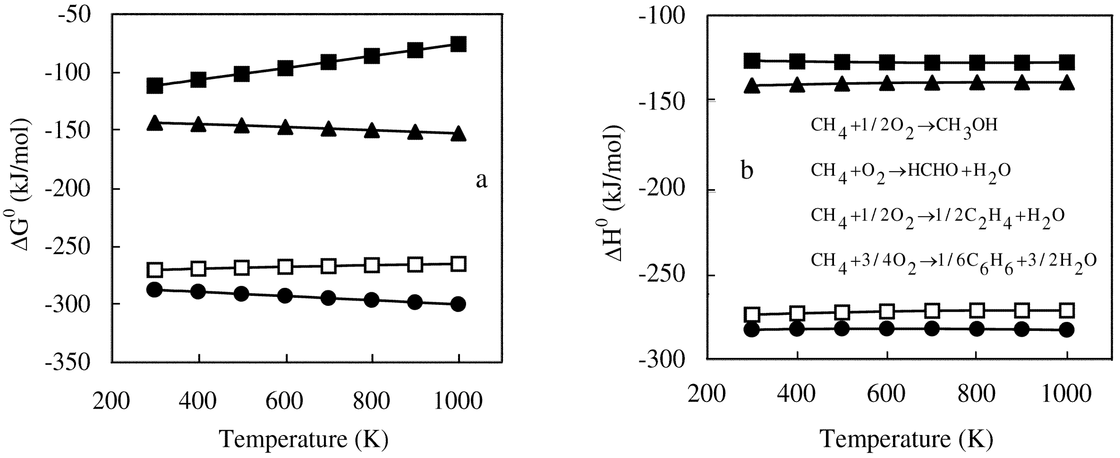

Figure 6. Variation of free energy change (a) and enthalpy change (b) with temperature for formation of various products (per mol of methane): CH_3OH, ■; HCHO, ●; C_2H_4, ▲; C_6H_6, □.

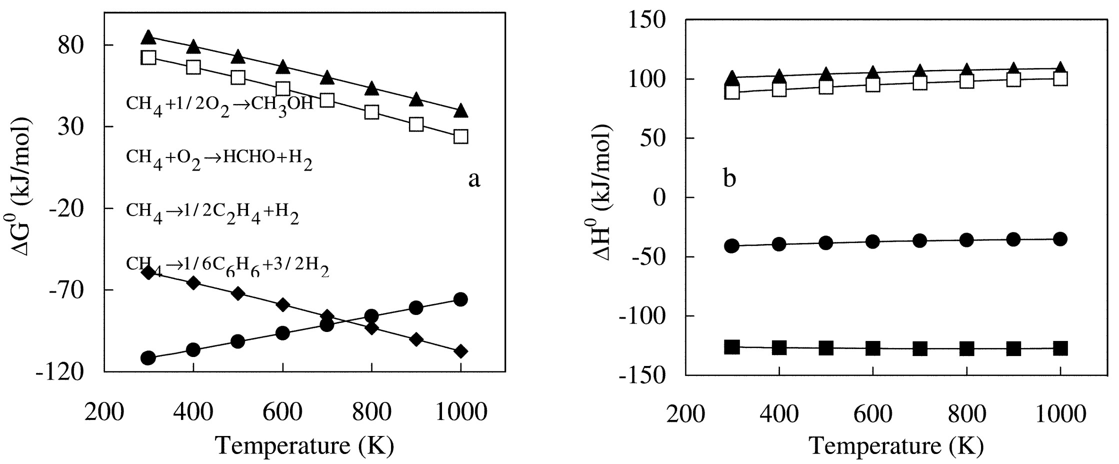

Figure 7. Variation of free energy change (a) and enthalpy change (b) with temperature for a series of reactions which lead to formation of hydrogen (per mol of methane): CH_3OH, ■; HCHO, ●; C_2H_4, ▲; C_6H_6, □.

mechanism proposed by Tabata *et al.* [9]. They suggested that CH_3 is first produced through reaction of CH_4 and NO_2, and CH_3 then reacts with NO_2 to produce CH_3NO_2 and *trans*-CH_3ONO, which decompose into a key intermediate, CH_3O. The free radical CH_3O reacts with O_2 or NO_x to produce HCHO, and with CH_4 to produce CH_3OH. The transition barriers of HCHO formation are lower than those for CH_3OH formation, and therefore higher temperatures are required for the latter. Our results show that HCHO begins to form at a temperature some 20 °C lower than that at which CH_3OH is first observed.

In our *in situ* spectra, no CH_3ONO or CH_3NO_2 was detected. It is noteworthy that Otsuka *et al.* reported a high selectivity to CH_3NO_2 (about 20%) with a CH_4/O_2 ratio of 2:1 at a temperature of 500 °C [7].

It should also be noted that neither of the mechanisms proposed by McConkey or Tabata can explain the formation of ethylene and aromatics in the products.

Thermodynamic analysis demonstrates that the formation of ethylene and benzene is more favorable relative to HCHO when the hydrogen atoms in the methane are partly converted to H_2O. It can be seen from figure 6 that in that case the formation of ethylene is actually slightly more thermodynamically favorable (in terms of both ΔH and ΔG) than that of CH_3OH. However, when the hydrogen atoms in the methane are partly converted to H_2, the formation of ethylene or benzene is not thermodynamically allowed even at temperatures above 800 °C, as shown in figure 7. In conclusion, the calculations and experimental results presented here strongly suggest that the formation of HONO is a key intermediate in the reaction studies and that formation of ethylene and aromatics needs to be considered in further mechanistic studies.

Acknowledgment

This project was supported by the Ministry of Science and Technology, China (G1999022202).

References

[1] T.E. Layng and R. Soukup, Ind. Eng. Chem. 20 (1928) 1052.
[2] B.H. McConkey and P.R. Wilkinson, I&EC Proc. Des. Dev. 6 (1967) 436.
[3] S. Irusta, E.A. Lombardo and E.E. Miró, Catal. Lett. 29 (1994) 339.
[4] L.B. Han, S. Tsubota and M. Haruta, Chem. Lett. (1995) 931.
[5] A.M. Bañares, J.H. Cardoso, G.J. Hutchings, J.M.C. Bueno and J.L.G. Fierro, Catal. Lett. 56 (1998) 149.
[6] K. Otsuka, R. Takahashi, K. Amakawa and I. Yamanaka, Catal. Today 45 (1998) 23.
[7] K. Otsuka, R. Takahashi and I. Yamanaka, J. Catal. 185 (1999) 182.
[8] P. Fornasiero, J. Kapar, S. Fagotto and M. Graziani, J. Catal. 189 (2000) 463.
[9] K. Tabata, Y. Teng, Y. Yamaguchi, H. Sakurai and E. Suzuki, J. Phys. Chem. A 104 (2000) 2648.
[10] J.H. Bromly, F.J. Barnes, S. Muris, X. You and B.S. Haynes, Combust. Sci. Technol. 115 (1996) 259.
[11] Z. Yan, H.-S. Shang, C.-X. Xiao and Y. Kou, ACS Symp. Ser. (in press).
[12] Z. Yan, C.-X. Xiao and Y. Kou, Catal. Lett. (in press).
[13] W.-T. Chan and H.O. Pritchard, PCCP 4 (2002) 557.